AppliedPhotophysics

Ultrasensitive Spectroscopy for the Life Sciences

Abstract Automated Circular Dichroism (ACD) was used to determine the thermodynamic stability of a protein by chemical denaturation.

▶ Incubation of samples ensures equilibrium is reached, eliminating systematic error;

▶ Short path lengths extend the accessible wavelength range;

▶ Automation significantly increases productivity and reduces human error.

Authors

SEBASTIAN FIEDLER

Graduate Student, Molecular Biophysics Group - University of Kaiserslautern

SANDRO KELLER

Head of Molecular Biophysics Group - University of Kaiserslautern

in cooperation with

LINDSAY COLE

Applications Development Manager - Applied Photophysics

www.photophysics.com/applications

Protein Stability by Chemical Denaturation

INTRODUCTION

Quantifying the stability of a protein is of fundamental importance in many areas of biomolecular research, including protein chemistry and protein engineering, protein–ligand and protein–protein interactions, as well as drug discovery and drug development. The thermodynamic stability of a protein is reflected in the change in Gibbs free energy, $\Delta G°$, characterising the equilibrium transition from a folded, native state to an ensemble of unfolded, denatured states, which usually do not posses biological activity. Thus, $\Delta G°$ is a key parameter for understanding the contributions to protein stability resulting from amino acid composition (hydrogen bonds, hydrophobic interactions, van der Waals contacts, salt bridges, aromatic interactions etc.), posttranslational modifications (glycosylation, methylation, etc.), or environmental factors (temperature, pressure, pH, salts, detergents, excipients etc.).

The primordial problem in quantifying protein stability is that, for most globular proteins under native conditions, typical values of $\Delta G°$ are so high that the unfolded state is scarcely populated. For instance, a value of $\Delta G°=40kJ/mol$, which is typical of medium-sized globular proteins, results in an equilibrium in which the folded state accounts for >99.99999% of total protein. Therefore, the minute amount of unfolded protein cannot be detected by most

KEYWORDS	
▶ Protein stability	▶ Automated circular dichroism
▶ Folded-unfolded equilibrium	▶ 96-well plate format
▶ Gibbs free energy $\Delta G°$	
▶ Chemical denaturants	

biophysical methods, and the folded–unfolded equilibrium cannot be determined directly. The solution to this problem consists in shifting the equilibrium away from the folded towards the unfolded state by changing the conditions such as to make the folded state less favourable, the unfolded state more favourable, or both. This can be achieved by different means, including an increase or decrease in pH or temperature or addition of chemical denaturants such as guanidinium chloride (GdnHCl) or urea (Street et al., 2008; Holthauzen et al., 2011). The $\Delta G°$ values measured under non-native conditions are then extrapolated back to native conditions, that is, physiological temperature or pH or zero denaturant concentration.

▶ **Thermal denaturation** is straightforward from a theoretical viewpoint because there exists a solid thermodynamic framework describing the dependence of $\Delta G°$ on temperature. Practically, this approach is convenient because a temperature ramp can be done in a sealed cuvette without changing the composition of the sample under investigation. However, many proteins tend to aggregate or precipitate at elevated temperature. Under such circumstances, resistance to thermal denaturation may be a valuable indicator of protein stability for comparative purposes, but it no longer fulfils the requirements for a rigorous thermodynamic interpretation (i.e. reversibility and absence of hysteresis). Moreover, the thermally denatured states of some, if not most, proteins retain considerably more secondary or even tertiary structure than their chemically unfolded states, which makes it impossible to ascribe changes in $\Delta G°$ exclusively to the biologically relevant folded states.

▶ **Chemical denaturants**, by contrast, are often capable of stabilising and solubilising unfolded polypeptide chains, thus rendering the unfolding reaction reversible by preventing aggregation and precipitation. However, chemical denaturation is more challenging than thermal denaturation from both theoretical and experimental viewpoints. This is, in part, because there is no rigorous thermodynamic link between $\Delta G°$ and the denaturant concentration. Empirically, it has been observed that the Gibbs free energy change depends linearly on denaturant concentration (Greene and Pace, 1974). This is expressed by the equation $\Delta G°(c_{denat}) = \Delta G°(0)-mc_{denat}$, where $\Delta G°(0)$ is the Gibbs free energy change in the absence of denaturant, which reflects the sought measure of protein stability under native conditions. The second fitting parameter reflects the dependence of the Gibbs free energy change on the denaturant concentration, $m=\partial\Delta G°/\partial c_{denat}$. This so-called m-value is usually interpreted to reflect changes in solvent-exposed protein surface area on unfolding. From a practical perspective, chemical denaturation experiments are cumbersome because they involve changes in solvent composition and therefore, unlike temperature ramps, cannot be carried out using a single sample enclosed in a sealed cuvette.

Chemical denaturation experiments can be carried out in either batch or titration mode, both of which are laborious, time-consuming, and prone to reproducibility problems if performed manually. Automated titrators have met with great success in the quantification of protein stability by chemical denaturation, because they allow for the unattended collection of numerous data points, increased throughput, and improved accuracy and precision resulting from the elimination of manual mixing steps (Street et al., 2008). Nevertheless, there remain a number of obstacles that limit the usefulness of titrators:

(1) *Slow equilibration:* most importantly, slowly equilibrating systems are not amenable to automated titration because the equilibration times required after each addition of denaturant would result in prohibitively lengthy titrations (Street et al., 2008; Holthauzen et al., 2011). Even among small, globular proteins, slow equilibration is rather common, which is most often due to peptidyl–prolyl cis–trans isomerisation (Kiefhaber, 1995). This is most severe for denaturant concentrations near the midpoint of the folded–unfolded transition. Since this is the concentration range where both the folded and the unfolded states are measurably populated, it is of paramount importance to avoid systematic errors resulting from insufficient sample equilibration. As an example, Figure 1 illustrates how the CD signal of hen egg white lysozyme approaches a new equilibrium value after dilution of folded protein into different concentrations of denaturant. For strongly denaturing conditions (7M GdnHCl), relaxation is accomplished within a couple of minutes. By contrast, if the final denaturant concentration is in the transition region (4M GdnHCl), the system requires much more time to equilibrate, thus invalidating the use of serial titrations for determining the thermodynamic stability of the protein.
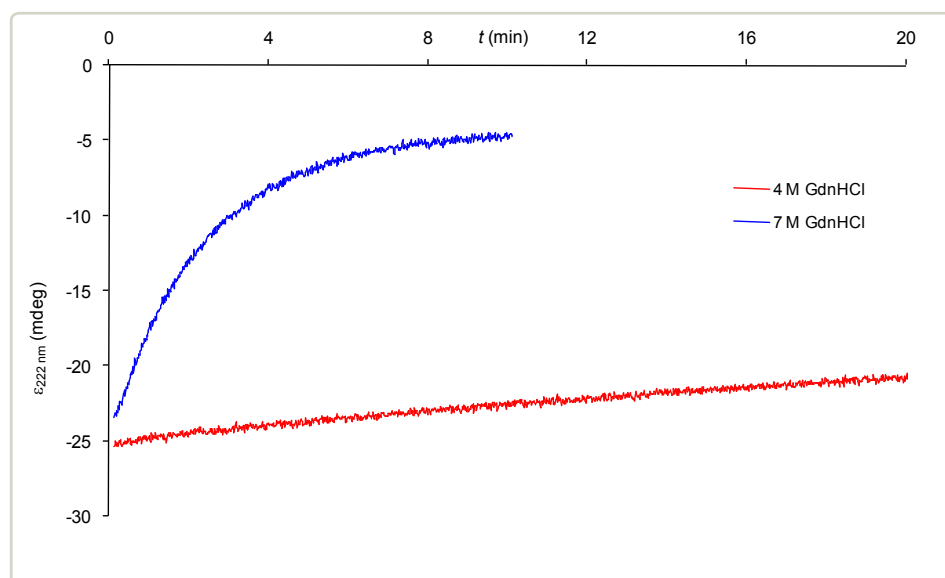

Figure 1. Kinetics of lysozyme unfolding at pH 3.5 near the transition midpoint (4M GdnHCl; red line) and under strongly denaturing conditions (7M GdnHCl; blue line).

(2) Long path lengths: after each addition of denaturant, the protein solution has to be stirred thoroughly, usually with the aid of a magnetic stir bar, to ensure complete mixing. This necessitates the use of cuvettes with volumes ≥500µL and light path lengths ≥4mm. The longer the path length is, the higher is the lowest wavelength at which the total absorbance of the sample is still in the acceptable range (typically, $A < 2$) and the shorter is the wavelength range observable by CD. This problem is particularly relevant to chemical unfolding experiments, because high concentrations of strongly absorbing denaturants further contribute to restricting the usable wavelength range. This becomes even more severe for membrane proteins, where light scattering from detergent micelles or lipid vesicles adds to the loss of low-wavelength light, as well as for β-sheet proteins, which above 230nm exhibit a rather small difference in the CD signal between the folded and the unfolded states.

(3) Lack of sample accessibility: another drawback of automated titrations is that the protein sample is accessible to scrutiny by other methods only before the titration experiment is started and once it is completed. In between the start (i.e. in the absence of denaturant) and the end (i.e. in the presence of very high denaturant concentrations) of the experiment, the sample composition or other properties cannot be studied using other methods. This is particularly critical for chemical denaturation experiments because the denaturant concentration is difficult to control accurately, which is due to differences in density, viscosity, and surface tension between concentrated denaturant solutions and aqueous buffer.

(4) Long exposure to UV light: finally, repeated measurements on the same protein sample in the presence of increasing concentrations of denaturant may lead to irreversible radiation damage due to prolonged exposure to UV light.

All of the above problems can be circumvented by **automated circular dichroism (ACD)** spectroscopy, that is, by performing CD measurements in batch rather than titration mode.

(1) Slowly equilibrating systems may be studied because many samples at various denaturant concentrations can be prepared and incubated in parallel before data acquisition, thus avoiding lengthy serial equilibration times between CD measurements.

(2) Since sample mixing is accomplished outside the optical cuvette before the actual experiment is initiated, the path length may be substantially shorter (down to 0.1mm), thus greatly extending the accessible wavelength range. With regard to sample consumption, the reduced cuvette volume also largely compensates for the fact that many samples have to be prepared in parallel.

(3) Each sample (i.e. the protein solution at each denaturant concentration) can be studied by other methods before or after the ACD experiment. For example, denaturant concentrations can be determined independently by refractometry over the whole concentration range rather than at the start and the end of the titration only.

(4) Each sample is exposed to UV light for only a short period of time.

MATERIALS AND METHODS

Hen egg white lysozyme, GdnHCl, and all other chemicals were obtained from Sigma–Aldrich. All experiments were performed in 50mM glycine buffer adjusted to pH 2.9. A denaturant stock solution was prepared by dissolving GdnHCl powder in 500mM glycine stock, adding triple-distilled water, heating the suspension to approximately 60°C, allowing it to cool to room temperature, adjusting the pH to 2.9, and finally adding triple-distilled water to reach the desired volume. The GdnHCl concentration in the stock solution was 7.96M, as determined by refractive index measurements on an Anton Paar Abbemat 500 refractometer using an empirical equation (Nozaki, 1972). A protein stock solution was prepared by dissolving lysozyme powder in buffer to yield a final protein concentration of 10mg/mL.

The ACD was programmed to prepare a series of 31 different GdnHCl concentrations ranging from 0 to 6M in increments of 200mM by mixing the GdnHCl stock solution with buffer. Each GdnHCl concentration was prepared in duplicate in two neighbouring wells, requiring a total of 62 wells out of the 96-well plate. After the automated preparation of the denaturant concentration series, each well contained a total volume of 1080μL, which was filled up to a final volume of 1200μL by manually adding either 120μL of the lysozyme stock solution (first well of each GdnHCl concentration duplicate) or the same volume of buffer (second well, blank). The solutions were mixed thoroughly and incubated for 4 hours at 20°C before the content of each well was split into three portions by transferring two times 400μL from each well of the master plate into corresponding wells on two other 96-well plates to create three replicates.

CD and absorbance spectra in the wavelength range of 200–320nm were recorded overnight in a fully automated, unattended fashion using a flow-through cell with a path length of 0.2mm, a step size of 1nm, and a spectral bandwidth of 1nm. The total digital integration time was 2.5s, which was split into 10 repeats of 0.25s each to enable the calculation of the standard deviation associated with the spectroscopic signal recorded at a particular wavelength and GdnHCl concentration. The temperature was adjusted to 20°C for both sample storage in 96-well plates and data acquisition in the flow-through cell. After automated CD and absorbance

measurements, the actual concentration of GdnHCl in each well was determined refractometrically as described above. Raw CD and absorbance spectra were corrected by subtracting blank spectra obtained without protein under otherwise identical conditions. Finally, blank-corrected CD spectra were normalised with respect to the absorbance at 217nm to account for variations in protein concentration, as described in detail below.
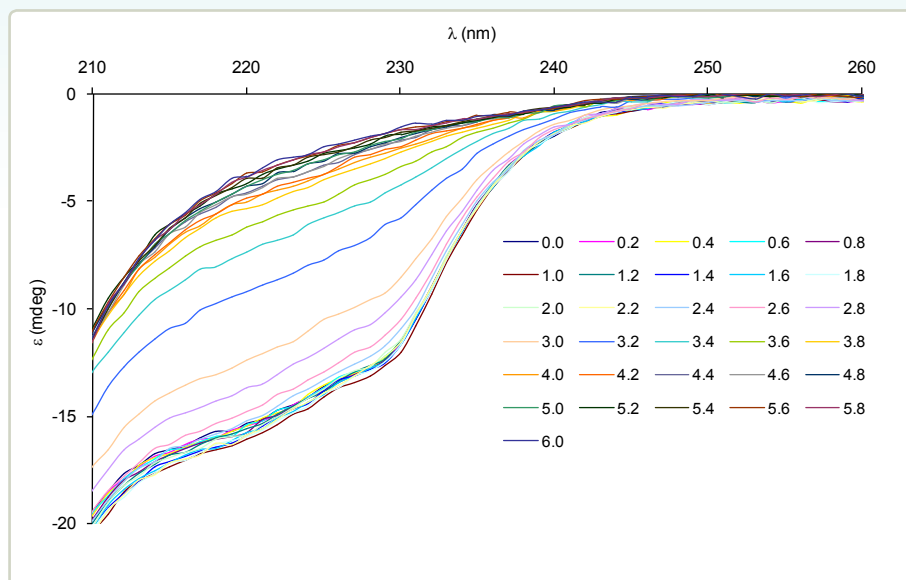
Figure 2. Blank-corrected CD spectra of 1mg/mL lysozyme at 31 different GdnHCl concentrations ranging from 0 to 6M (see legend).

RESULTS & DISCUSSION

Figure 2 shows CD spectra obtained from solutions containing 1mg/mL lysozyme and GdnHCl, whose concentration was increased from 0 to 6M in increments of 200mM. Denaturant-induced protein unfolding is reflected in a strong decrease in the absolute ellipticity below 240nm. The most dramatic changes in signal intensity occur in the wavelength range of 215–230nm, where upon unfolding the pronounced CD signatures of native lysozyme give way to rather weak signals characteristic of an unordered polypeptide. Plotting the ellipticity at 222nm versus the GdnHCl concentration yields the unfolding isotherm depicted in Figure 3. From both the CD spectra and the isotherm, it is obvious that the major changes in secondary structure and, thus, in the folded–unfolded equilibrium occur around 3M GdnHCl. In the pre-transition baseline (below 2M GdnHCl) and in the post-transition baseline (above 4M GdnHCl), only minor changes are apparent. The small positive slope in the post-transition baseline results from an expansion of the denatured-state ensemble and a concomitant loss of residual secondary structure with increasing GdnHCl concentration. By contrast, variations in the pre-transition baseline appear random. As can be deduced from the very small standard deviations of the ellipticity values plotted in Figure 3, these variations cannot be due to uncertainties inherent in the spectroscopic signal itself. Rather, the most likely source of the scatter in the signal intensity are variations in the protein

concentration, which are expected to be more pronounced at low denaturant concentrations.

Such effects can be corrected for by normalising the ellipticity data with respect to the absorbance, which is recorded along with the CD signal. In doing so, however, it should be realised that the absorbance itself may depend on the conformation of the protein as well as on solvent conditions (i.e. GdnHCl concentration) and thus need not be proportional to the protein concentration.
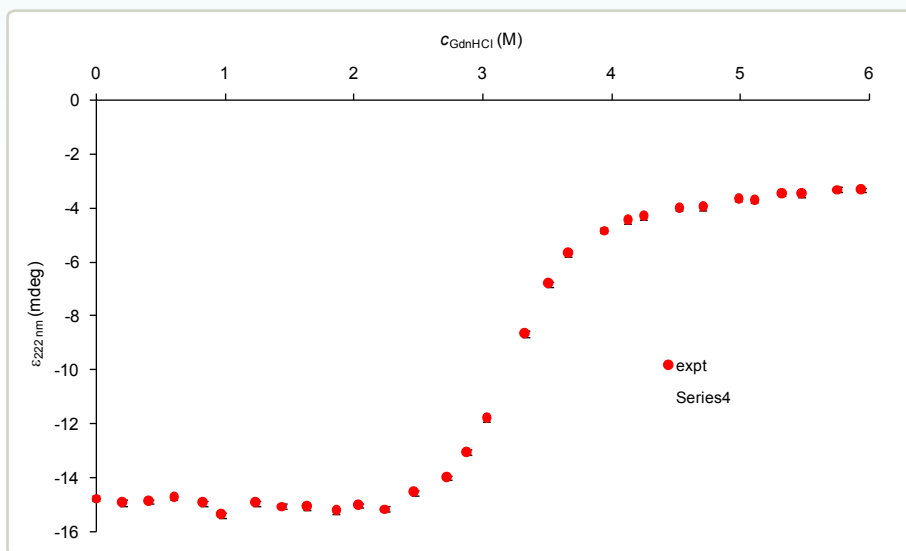

Figure 3. Unfolding isotherm obtained by plotting the ellipticity at 222nm (from Figure 2) as a function of GdnHCl concentration. Experimental data (red dots) with standard deviations (black bars).
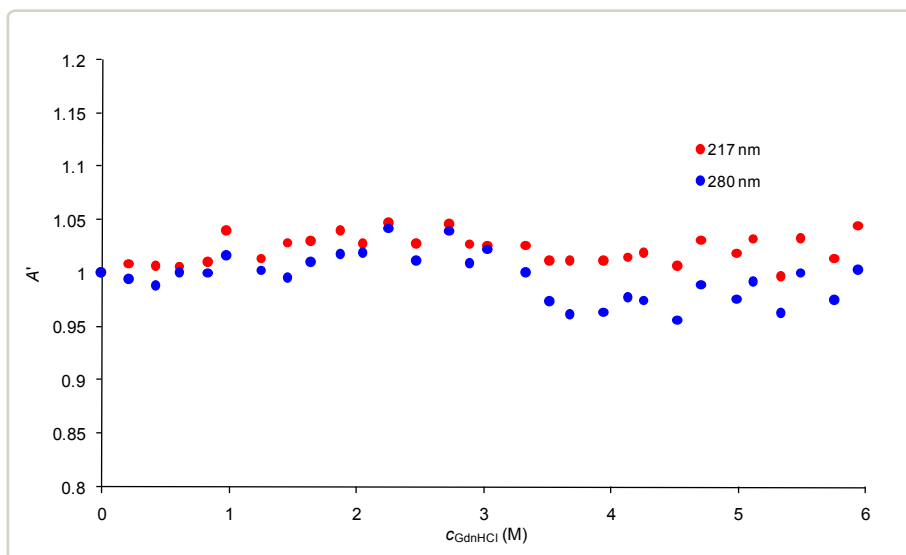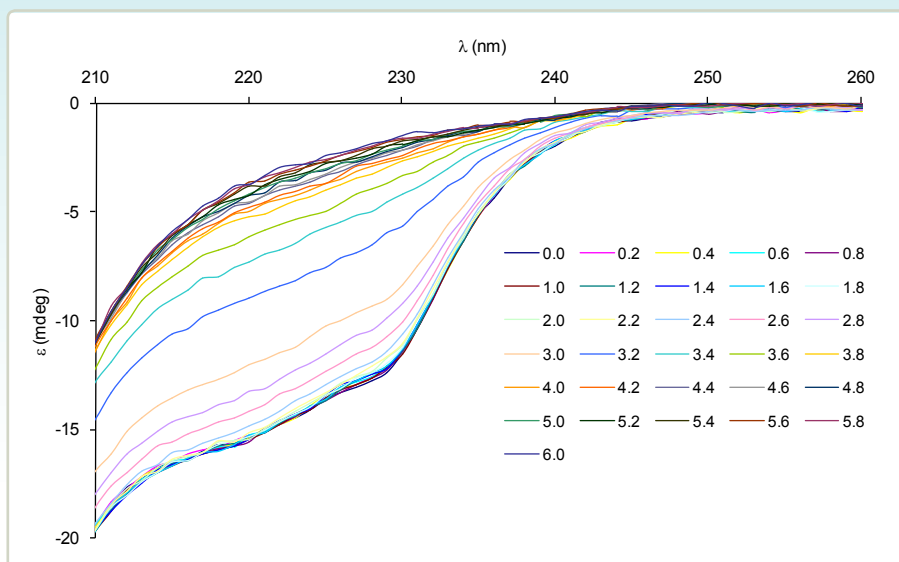

Figure 4. Relative absorbance values at 217nm (red symbols) and 280 nm (blue symbols) as a function of GdnHCl concentration. For ease of comparison, all values were scaled relative to the absorbance in the absence of GdnHCl.

Figure 5. Normalised CD spectra of 1mg/mL lysozyme at 31 different GdnHCl concentrations ranging from 0 to 6M (see legend). Blank-corrected CD spectra (from Figure 2) were normalised with respect to the absorbance at 217nm (see text for details).

For instance, normalising the CD spectra on the basis of the absorbance at 280nm, which is often used to determine protein concentrations spectrophotometrically, would introduce a systematic error because the absorbance at this wavelength is significantly affected by the conformational change on unfolding. This can be seen in Figure 4 as a systematic decrease of the absorbance in the transition region around 3M GdnHCl. However, there exist a number of other wavelengths for which this is not the case. Under the conditions used in this study, we found the absorbance at 217nm not to depend systematically on the GdnHCl concentration, as also shown in Figure 4.

Normalising the ellipticity values in Figures 2 and 3 with respect to the absorbance at 217nm produces the CD spectra and the unfolding isotherm in Figures 5 and 6, respectively. The normalised CD spectra in the pre-transition region (below 2M GdnHCl) overlay in Figure 5, which also manifests itself in an improved signal-to-noise ratio in the unfolding isotherm in Figure 6. It should be noted that normalisation has a significant effect also on the crucial data points in the transition region in Figure 6, which is, however, less obvious to visual inspection because there are large point-to-point differences in this part of the isotherm where the equilibrium shifts from the folded to the unfolded state.
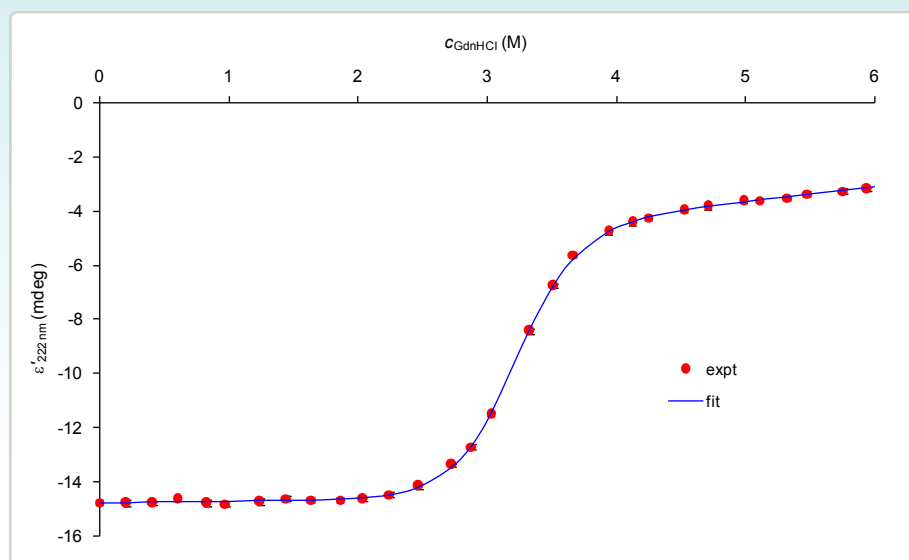
Figure 6. Unfolding isotherm obtained by plotting the absorbance-normalised ellipticity at 222nm (from Figure 5) as a function of GdnHCl concentration. Experimental data (red dots) with standard deviations (black bars) and fit according to Eqn.1 (blue line).

Also shown in Figure 6 is a fit to the experimental data using a standard equation (Street et al., 2008; Holthauzen et al., 2011) based on the observation that both $\Delta G°$ as well as the ellipticities in the pre- and post-transition baselines change linearly with the GdnHCl concentration. Since each data point in the unfolding isotherm comes with its standard deviation, weighted nonlinear least-squares analysis (Johnson, 1992) can be used to obtain the best-fit parameters of $\Delta G°$ and m. Moreover, the reliability of this fitting procedure can be assessed by estimating the standard deviations from the 68.3% confidence intervals derived from error surface projections, as explained in detail elsewhere (Kemmer and Keller, 2010). Applying this approach to the data depicted in Figure 6 yielded $\Delta G°=(32.5\pm1.1)$ kJ/mol and $m=(10.1\pm0.7)$ kJ/(mol M) for the best-fit values and standard deviations of the two thermo dynamic parameters of interest.

The narrow error margins of $\Delta G°$ are remarkable, as this value is often associated with considerable uncertainty due to a long extrapolation from the transition region to zero denaturant. It should be noted that the above-mentioned analysis based on error surface projections is more rigorous than other approaches typically used by commercial data analysis software, which would yield even narrower (but usually unrealistically narrow) error margins. Obtaining precise $\Delta G°$ values is crucial because changes in amino acid composition or environmental factors, such as the presence of excipients or other co-solutes, oftentimes have significant but subtle effects on the stability of the protein under study.

The error margins of both $\Delta G°$ and m can be further narrowed down by simultaneously fitting ellipticity values collected at several different wavelengths from the existing dataset or by decreasing the increment in the GdnHCl concentration and measuring more data points per isotherm. Importantly, the application of nonlinear least-squares methods is valid only if the uncertainty in the x-axis (i.e. GdnHCl concentration) is negligible in comparison with that in the y-axis (i.e. normalised ellipticity). The very good signal-to-noise ratio in Figure 6 therefore emphasises the necessity of determining the denaturant concentration in each sample accurately and independently, which would not be possible in a classical titration experiment. Finally, Table 1 underscores the excellent reproducibility of chemical protein denaturation studies using ACD by summarising the results of five independent experiments performed under identical conditions.

	$\Delta G°$ (kJ/mol)		m (kJ/(mol M))	
	best-fit value	standard deviation*	best-fit value	standard deviation*
Experiment 1	32.0	1.6	9.8	0.9
Experiment 2	32.0	1.2	9.7	0.8
Experiment 3	31.6	1.2	9.7	0.8
Experiment 4	30.9	1.0	9.6	0.6
Experiment 5	32.6	1.3	10.3	0.8

Table 1. Obtained from 68.3% confidence intervals by error surface projection.

REFERENCES

Greene and Pace. Urea and guanidine hydrochloride denaturation of ribonuclease, lysozyme, α-chymotrypsin, and β-lactoglobulin. *J. Biol. Chem*. **1974**, *249*, 5388–5393.

Holthauzen, Auton, Sinev, and Rösgen. Protein stability in the presence of cosolutes. *Methods Enzymol*. **2011**, *492*, 61–125.

Johnson. Why, when, and how biochemists should use least squares. *Anal. Biochem*. **1992**, *206*, 215–225.

Kemmer and Keller. Nonlinear least-squares data fitting in Excel spreadsheets. *Nat. Protoc*. **2010**, *5*, 267–281.

Kiefhaber. Kinetic traps in lysozyme folding. *Proc. Natl. Acad. Sci. USA* **1995,** *92*, 9029–9033.

Nozaki. The preparation of guanidine hydrochloride. *Methods Enzymol.* **1972**, *26*, 43–50.

Street, Courtemanche, and Barrick. Protein folding and stability using denaturants. *Methods Cell Biol*. **2008**, *84*, 295–325.

AppliedPhotophysics

Ultrasensitive Spectroscopy for the Life Sciences

4210Q258 v.4

Applied Photophysics Ltd,
21, Mole Business Park, Leatherhead, Surrey, KT22 7BA, UK
Tel (UK): +44 1372 386 537
Tel (USA): 1-800 543 4130
Fax: +44 1372 386 477

Applied Photophysics was established in 1971 by
The Royal Institution of Great Britain

www.photophysics.com/applications